

# Reactivity and Stereoselectivity of $6\pi$ and Nazarov Electrocyclizations of Bridged Bicyclic Trienes and Divinyl Ketones

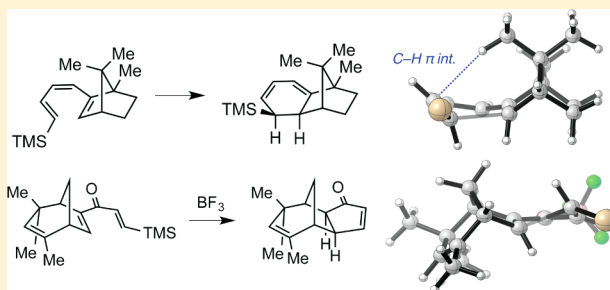
Ashay Patel,<sup>†</sup> F. G. West,<sup>‡</sup> and K. N. Houk<sup>\*,†</sup>

<sup>†</sup>Department of Chemistry and Biochemistry, University of California, Los Angeles, California 90095, United States

<sup>‡</sup>Department of Chemistry, University of Alberta, Edmonton, AB T6G 2G2, Canada

**S** Supporting Information

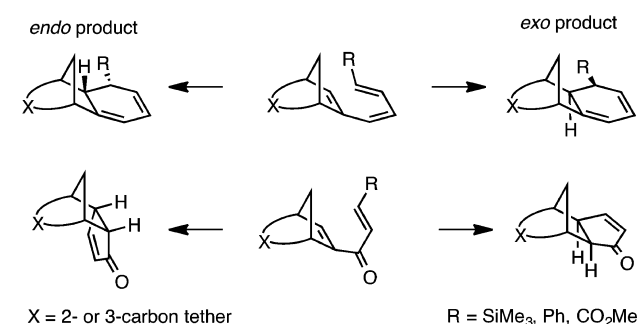
**ABSTRACT:** The  $6\pi$  electrocyclizations and Nazarov cyclizations of a series of bridged bicyclic substrates were modeled with the M06-2X density functional and the def2-TZVPP basis set, and the factors responsible for the reactivities of these substrates and the stereoselectivities of their ring closures were identified. The ring closures of these bridged bicyclic trienes are up to a million-fold faster ( $\Delta\Delta G^\ddagger = 10 \text{ kcal mol}^{-1}$ ) than that of 1,3,5-hexatriene, despite the absence of any activating functional groups. Three effects, preorganization, predistortion, and a CH  $\pi$  interaction, are responsible for this sizable difference in reactivity. Stereoselectivity is partially controlled by torsional effects, but for highly *exo* selective electrocyclizations, it is reinforced by a second effect (either a CH  $\pi$  interaction or a steric clash). The absence of this second effect in the ring closures of several divinyl ketones explains the reduced selectivity of these ring closures. In one case, a divinyl ketone (ketone **6**) undergoes Nazarov cyclization to yield the *endo* product preferentially. For this example, through-space interaction of a nonconjugated alkene with the divinyl ketone  $\pi$  system in the *endo* transition state and a steric effect override the intrinsic *exo* selectivity.



## INTRODUCTION

West et al. have prepared a series of bridged bicyclic trienes<sup>1</sup> and divinyl ketones<sup>2,3</sup> that undergo highly stereoselective triene ( $6\pi$ ) electrocyclizations and Nazarov cyclizations. These bicyclic substrates are shown in Scheme 1. Carbatriene<sup>4–9</sup>

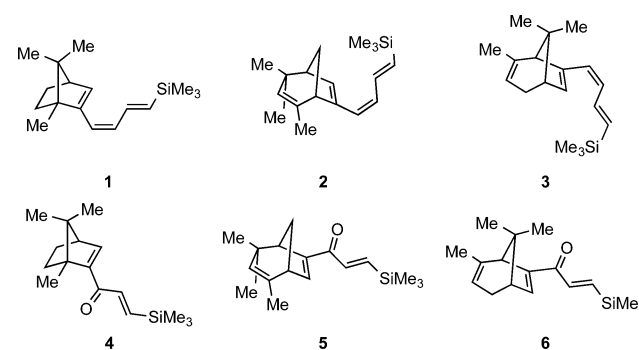
**Scheme 1.  $6\pi$  and Nazarov Electrocylation of Bridged Bicyclic Trienes and Divinyl Ketones**



and Nazarov electrocyclizations<sup>10–25</sup> have been the subject of prior computational studies, but the ring closures of bridged bicyclic substrates like those shown in Scheme 2 have yet to be examined computationally.

The electrocyclic reactions of these bridged bicyclic trienes and divinyl ketones merit computational study because (1) the bridged bicyclic trienes react with surprising ease when

**Scheme 2. Experimental Substrates Examined Computationally in This Study**



compared to that of their acyclic counterpart, 1,3,5-hexatriene, and (2) these bridged bicyclic trienes and divinylketones undergo ring closure with (often high) *exo* selectivity.

We have discovered that the enhanced reactivity of these bicyclic trienes toward disrotatory ring closure is due to three factors: substrate preorganization, predistortion, and a CH  $\pi$  interaction. Each of these effects individually has a modest impact on the rate of reaction, but, taken together, these effects are, according to computations, responsible for up to a  $\sim 10^6$ -fold (at 298.15 K) increase in the rate of ring closure relative to

Received: January 11, 2015

Published: January 29, 2015

that of 1,3,5-hexatriene. This explains why the triene precursor, generated *in situ*, is never observed experimentally. The *exo* selectivities of both the Nazarov and triene ring closures are consistent with the observed stereoselectivity of (cyclo)-additions involving bridged bicyclic alkenes, including norbornene,<sup>26–32</sup> and are controlled by torsional effects.<sup>33–37</sup> However, no investigation of the role of such effects on electrocyclization stereoselectivities has been reported. Our results suggest that, unlike (cyclo)additions to bicyclic substrates, high *exo* selectivity in the electrocyclizations of bridged bicyclic substrates 1–6 requires a second stereocontrol element in addition to such torsional effects. In the examples reported here, either a CH  $\pi$  interaction or steric repulsion can also promote *exo* stereoselectivity. By contrast, divinyl ketone 6 reacts to form the *endo* product because participation of a nonconjugated alkene stabilizes the *endo* transition state, overcoming the intrinsic preference for the *exo* product.

## RESULTS AND DISCUSSION

**Reactivities of Bridged Bicyclic Trienes toward  $6\pi$  Electrocyclizations.** The M06-2X/def2-TZVPP computed  $\Delta G^\ddagger$  of 31.5 kcal mol<sup>-1</sup> for the ring closure of 1,3,5-hexatriene is in good agreement with the experiment value of 29.9 kcal mol<sup>-1</sup>.<sup>38</sup> Unlike the electrocyclization of 1,3,5-hexatriene, bridged bicyclic trienes 1–3 shown in Scheme 2 undergo spontaneous ring closure upon formation.<sup>1</sup> According to our calculations, the ring closure of bicyclic triene 1 has a  $\Delta G^\ddagger$  of 21.4 kcal mol<sup>-1</sup>, roughly 10 kcal mol<sup>-1</sup> lower than the computed  $\Delta G^\ddagger$  for the ring closure of 1,3,5-hexatriene.<sup>38</sup>

The effects responsible for the unusual reactivities of these bicyclic trienes were ascertained using the series of model reactions shown in Figure 1. 1,2-disubstituted triene 9 is ~100-

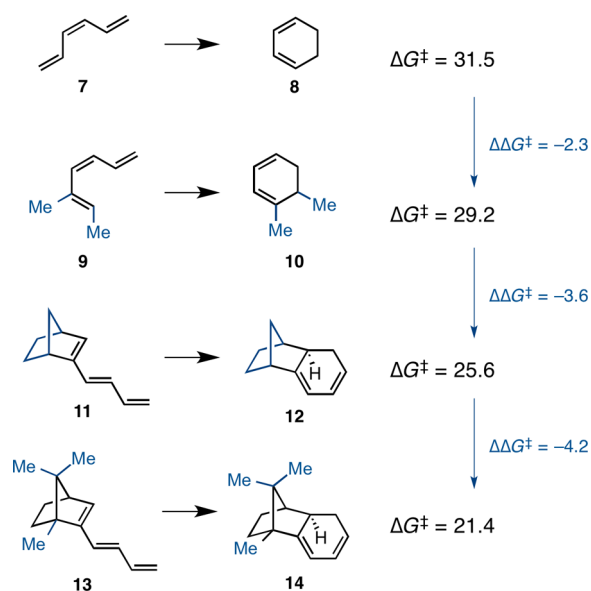


**Figure 1.**  $\Delta G^\ddagger$  of the electrocyclizations of model trienes 7, 9, 11, and 13. M06-2X/def2-TZVPP free energies are reported in kcal mol<sup>-1</sup>.

fold more reactive (at room temperature) than unsubstituted triene 7 because the C2 methyl group destabilizes the *s-trans*, *s-trans* conformer by introducing an allylic clash in this conformer, as shown in Figure 2. This effect is apparent in all 1,2-disubstituted trienes described here and has also been

observed in the intramolecular Diels–Alder reactions of bicyclic 1,3,9-trienes.<sup>39</sup>

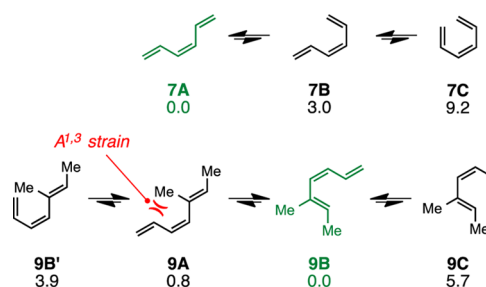


**Figure 2.** Conformational preferences of trienes 7 and 9. Relative stabilities ( $\Delta G$ ) of various conformers determined using M06-2X/def2-TZVPP. Energy values are reported in kcal mol<sup>-1</sup>.

The difference between the  $\Delta G^\ddagger$  (ca. 2.8 kcal mol<sup>-1</sup>) values for disubstituted trienes 9 and 11 can be attributed to predistortion of the endocyclic alkene of the norbornenyl substrate;<sup>40</sup> the strained nature of norbornenyl double bond is well-documented, and alkene predistortion of this sort has been known to contribute to norbornene's unusual reactivity in (cyclo)additions.<sup>33–37</sup> This effect likely also contributes to the enhanced reactivities of trienes 2 and 3. Lastly, a CH  $\pi$  interaction between the CH bond of the 7-methyl group and the triene  $\pi$  system further lowers the activation barrier for ring closure by 4.2 kcal mol<sup>-1</sup> for 6,7,7-trimethyl derivative 13 relative to unsubstituted norbornenyl triene 11 (Figure 3). This

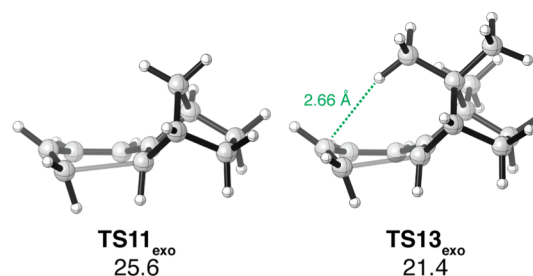


**Figure 3.** Transition structures and  $\Delta G^\ddagger$  (M06-2X/def2-TZVPP values are reported in kcal mol<sup>-1</sup>) of the *exo* ring closures of trienes 11 and 13, illustrating the stabilizing CH  $\pi$  interaction responsible for the enhanced reactivity of triene 13 relative to that of 11. Energies are M06-2X/def2-TZVPP  $\Delta G^\ddagger$  reported in kcal mol<sup>-1</sup>.

value is in line with theoretical<sup>41–43</sup> and experimental<sup>41</sup> values (ca. 1.0 of the CH  $\pi$  interaction found in the benzene–methane dimer);<sup>44</sup> the *exo* ring closure of triene 2, which possesses no methyl group on the bridge, has an activation free energy 1 kcal mol<sup>-1</sup> higher than that of triene 1. The Supporting Information describes further evidence of this CH  $\pi$  interaction by way of additional model computations.

**Stereoselectivities of the Disrotatory Ring Closures of Bridged Bicyclic Trienes.** The experimental and computed diastereomeric ratios of the triene electrocyclizations of bicyclic trienes 1–3 are summarized in Figure 4. Theory quantitatively reproduces the *exo* selectivity observed experimentally for the ring closures of 1–3.

Torsional steering, or minimization of torsional repulsions in transition states, at least partially controls the stereoselectivities of all electrocyclizations described in this article. The *endo* and *exo* transition states for the ring closure of camphor-derived

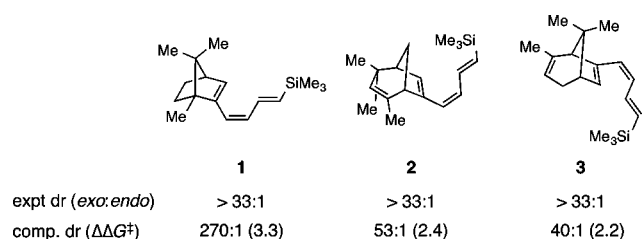


**Figure 4.** Computed and experimental diastereomeric ratios for the ring closures of triene 1–3. Reactions performed in aqueous THF at room temperature or under reflux in either THF/H<sub>2</sub>O or CH<sub>2</sub>Cl<sub>2</sub>. Computed diastereomeric ratios determined using the SMD<sup>THF</sup>/M06-2X/def2-TZVPP model chemistry.

triene 1, shown in Figure 5, illustrate the nature of this effect. The H–C–C–H dihedral shown in Figure 5 is staggered (63°)

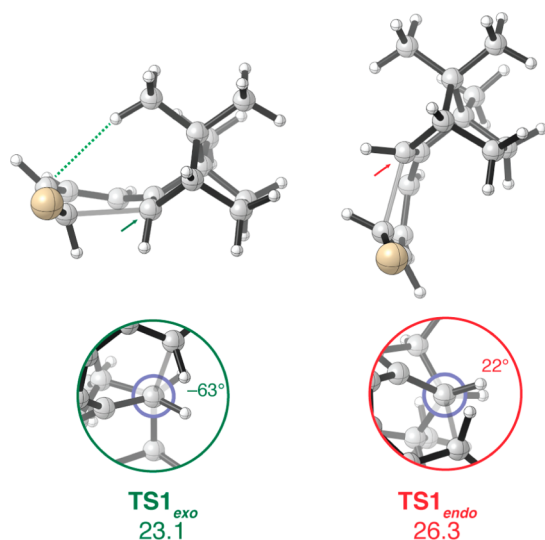


**Figure 5.** Transition structures and  $\Delta G^\ddagger$  (SMD<sup>THF</sup>/M06-2X/def2-TZVPP values are in kcal mol<sup>-1</sup>) for the *exo* and *endo* modes of ring closure of bicyclic triene 1. Methyl groups of the trimethylsilyl substituent are omitted for clarity.

in TS1<sub>exo</sub> and more eclipsed (21°) in TS1<sub>endo</sub>, leading to increased torsional strain in the *endo* transition state. The energy difference between the *endo* and the *exo* transition states of model triene 11 suggest that this effect accounts for roughly half of the 3 kcal mol<sup>-1</sup> difference in the free energies of TS1<sub>exo</sub> and TS1<sub>endo</sub>. Thus, a second effect must reinforce the intrinsic *exo* selectivity of the electrocyclizations of these bridged bicyclic trienes. In the case of trienes 1 and 3, this second effect is a stabilizing CH  $\pi$  interaction (described previously) between the 7-methyl substituent and the triene  $\pi$  system in the *exo* transition state.

Unlike trienes 1 and 3, triene 2 is unsubstituted at the bridging carbon; therefore, the CH  $\pi$  interaction described previously cannot act as a stereocontrol element for the electrocyclization of this substrate. Nevertheless, according to our DFT results, the  $\Delta G^\ddagger$  difference between TS2<sub>endo</sub> and TS2<sub>exo</sub> is 3 kcal mol<sup>-1</sup>. Interestingly, the barrier for the formation of the *endo* product of 2 is roughly 3 kcal mol<sup>-1</sup> higher than the  $\Delta G^\ddagger$  computed for the *endo* ring closures of bicyclic trienes 1 and 3, suggesting that a second destabilizing effect present in TS2<sub>endo</sub> is responsible for enhancing *exo* selectivity. Ring closure from the *endo* face is further

destabilized by a severe steric clash (shown in Figure 6) between the methyl substituent on the bicyclic skeleton and the

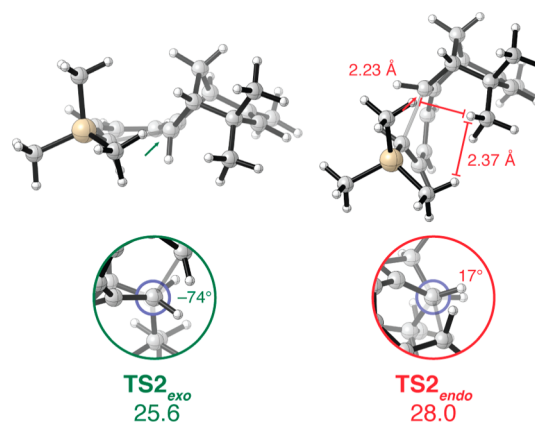


**Figure 6.** Transition structures and  $\Delta G^\ddagger$  (SMD<sup>THF</sup>/M06-2X/def2-TZVPP values are in kcal mol<sup>-1</sup>) for the *exo* and *endo* modes of ring closure of bicyclic triene 2. Methyl groups of trimethylsilyl substituent are shown to illustrate the steric clash that destabilizes the *endo* transition state.

hydrogen at the exocyclic terminus of the triene  $\pi$  system, as suggested by West in his initial report.<sup>1</sup> The two clashing hydrogens are separated by only 1.90 Å.

**Stereoselectivities of the Conrotatory Ring Closures of Bridged Bicyclic Divinyl Ketones.** The computed drs (Figure 7) for the Nazarov cyclization of divinyl ketone 4–6

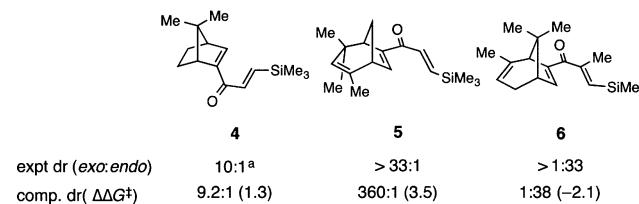


**Figure 7.** Computed and experimental diastereomeric ratios for the ring closures of divinyl ketones 4–6 in dichloromethane. Reactions performed in CH<sub>2</sub>Cl<sub>2</sub> at -78 °C to room temperature. Computed diastereomeric ratios determined using the SMD<sup>DCM</sup>/M06-2X/def2-TZVPP model chemistry.

are also in quantitative agreement with experiment. These ring closures were modeled with BF<sub>3</sub>, the Lewis acid employed experimentally, coordinated to carbonyl oxygens of the divinyl ketones.

The electrocyclic reaction of camphor-derived divinyl ketone 4 ( $\Delta\Delta G^\ddagger = 1.3$  kcal mol<sup>-1</sup>) is less selective than the ring closure of triene 1 because the conrotatory *exo* transition state is not stabilized by a CH  $\pi$  interaction (Figure 8). Unlike the 6-carbon  $\pi$  system of the corresponding triene system, the (formal) pentadienyl reactive array of divinyl ketone 4 adopts an arrangement in which its  $\pi$  density is directed away from the bridging methyl group. Consequently, the selectivity is exclusively determined by torsional effect, which amounts to a 1.1 kcal mol<sup>-1</sup> difference in  $\Delta G^\ddagger$  of the two modes of ring closure.

The stereochemical outcome of the Nazarov cyclization of bicyclic divinyl ketone 5 is controlled by the same effects responsible for the ring closure of triene 2, namely, torsional strain and steric repulsion destabilize the *endo* transition state of

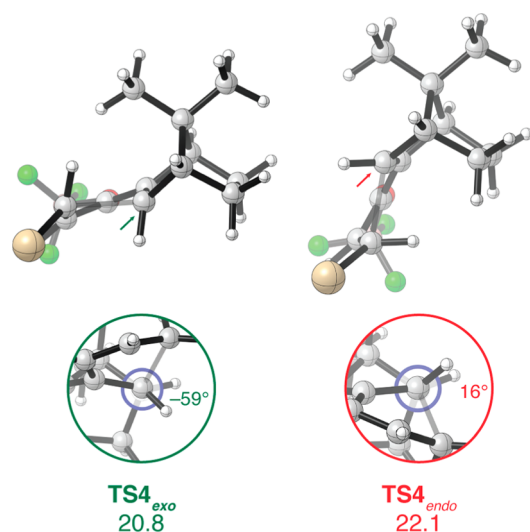


**Figure 8.** Transition structures and  $\Delta G^\ddagger$  (SMD<sup>DCM</sup>/M06-2X/def2-TZVPP values are in kcal mol<sup>-1</sup>) for the *exo* and *endo* modes of ring closure of bicyclic divinyl ketone **4**. Methyl groups of the trimethylsilyl substituent are omitted for clarity.

this reaction. The steric repulsion between the trimethylsilyl group and the remote bridge of the bicyclic system is diminished in the *endo* transition state of **4** as compared to that in **1** due to the decreased steric demand of the 3-carbon unsaturated ketone side chain relative to the 4-carbon diene side chain of **1**. See the Supporting Information for the transition structures and  $\Delta G^\ddagger$ 's for Nazarov cyclizations of **5**.

In contrast to the results already described, divinyl ketone **6** undergoes electrocyclization to form the *endo* product selectively. The transition states for the ring closure of this substrate are shown in Figure 9. Computations recapitulate the sense and level of stereoselectivity observed experimentally ( $\Delta\Delta G^\ddagger = 2.1$  kcal mol<sup>-1</sup>). West et al. proposed that a through-space orbital interaction involving the nonconjugated alkene at C5–C6 (labeled in Figure 10) and the 4-electron  $\pi$  system stabilizes the *endo* transition state, overriding the intrinsic *exo* selectivity. We find that this through-space interaction is partly

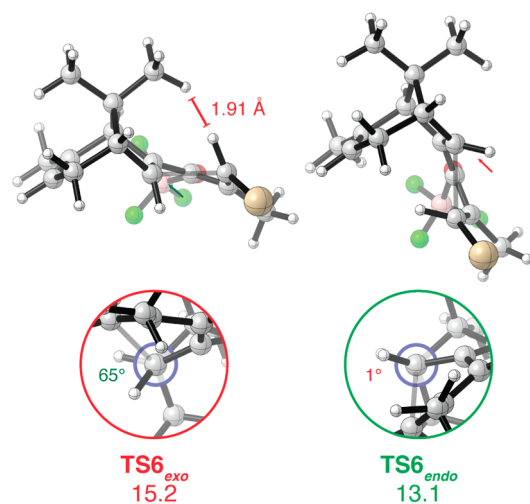


**Figure 9.** Transition structures and  $\Delta G^\ddagger$  (SMD<sup>DCM</sup>/M06-2X/def2-TZVPP values are in kcal mol<sup>-1</sup>) for the *exo* and *endo* modes of ring closure of bicyclic divinyl ketone **6**. Methyl groups of the trimethylsilyl substituent are omitted for clarity.

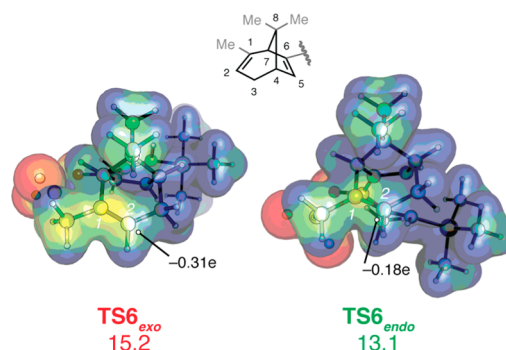


**Figure 10.** Molecular electrostatic potentials (MEPs) for  $TS6_{endo}$  and  $TS6_{exo}$  and  $\Delta G^\ddagger$ . Potential ranges from  $-0.5$  to  $0.5$  au. CHelpG atomic charges at C2 (the distal carbon of the nonconjugated alkene) are labeled in black. Molecular electrostatic potentials, densities, and  $\Delta G^\ddagger$  were determined using SMD<sup>DCM</sup>/M06-2X/def2-TZVPP.

responsible for the *endo* selectivity and that this effect is stronger in the *endo* transition state, as the  $\pi$  system of the pentadienyl cation is more ideally positioned to interact with the nonconjugated alkene. Computations show that the distance between the interacting carbon atoms (C1 and C6) is  $0.15$  Å shorter in  $TS6_{endo}$  than  $TS6_{exo}$ . Furthermore, the molecular electrostatic potentials (MEPs) show that the nonconjugated alkene is more electron-rich in the *exo* transition structure (more yellow in color) than in the *endo* transition structure (more green in color). The atomic charge on the distal carbon (C2) of the nonconjugated alkene is less negative in  $TS6_{endo}$  ( $-0.18e$ ) than in  $TS6_{exo}$  ( $-0.31e$ ), also indicative of greater interaction in  $TS6_{endo}$ . In addition, *endo* selectivity is enhanced by a steric clash that destabilizes the *exo* transition of **6**. A severe clash ( $1.91$  Å) exists between the methyl substituent at bridging carbon and the hydrogen at the exocyclic terminus of the  $\pi$  system (shown in Figure 9). We have examined a model substrate in which the (interacting) nonconjugated alkene has been saturated. For this substrate, *exo* selectivity is observed, in support of our hypothesis. See the Supporting Information for further details.

## CONCLUSIONS

Substrate preorganization, predistortion, and steric attraction emerge as factors that can promote the electrocyclic reaction of 1,3,5-hexatrienes. Torsional effects alone do not account for the level of selectivity observed for these ring closures; high *exo* selectivity requires the complementary action of a second effect (steric attraction or repulsion). In one system, **6**, through-space interaction of a nonconjugated alkene and steric repulsions reverse the intrinsic *exo* selectivity of Nazarov cyclization.

## COMPUTATIONAL METHODS

All quantum mechanical calculations were performed using Gaussian09.<sup>45</sup> Geometry optimizations and frequency calculations were performed with the hybrid meta-GGA density functional M06-2X<sup>46</sup> and the def2-TZVPP<sup>47</sup> basis set. The SMD solvation model<sup>48</sup> was used for the reactions of trienes **1–3** and divinyl ketones **4–6** in THF and CH<sub>2</sub>Cl<sub>2</sub>, respectively. For all calculations, we employed an ultrafine integration grid consisting of 99 radial shells and 590 angular points per shell. Normal mode analysis confirmed all stationary points as being either minima or transition states. Unscaled M06-2X/def2-TZVPP frequencies were used to calculate Helmholtz enthalpies and Gibbs free energies at 25 °C and 1 atm. Truhlar's quasiharmonic approximation was used to correct for errors in the estimation of vibrational entropies due to treatment of low modes (below 100 cm<sup>-1</sup>)

as harmonic oscillations. Molecular electrostatic potentials were rendered using the PyMOL Molecular Graphics System.<sup>49</sup> Gauss-View<sup>50</sup> and Avogadro<sup>51,52</sup> were used to construct and visualize structures. Structures were rendered using CYLview software.<sup>53</sup>

## ■ ASSOCIATED CONTENT

### ■ Supporting Information

Cartesian coordinates, electronic energies, zero point energy, and thermal corrections for all reported structures; imaginary frequencies for transition states; discussions and illustrations of the transition states for the ring closures of substrates **3** and **5**; and additional computational details. This material is available free of charge via the Internet at <http://pubs.acs.org>.

## ■ AUTHOR INFORMATION

### Corresponding Author

\*E-mail: [houk@chem.ucla.edu](mailto:houk@chem.ucla.edu).

### Notes

The authors declare no competing financial interest.

## ■ ACKNOWLEDGMENTS

K.N.H and F.G.W. acknowledge the NSF (CHE 105 9084 and CHE 136 1104 to K.N.H.) and the Natural Sciences and Engineering Research Council of Canada (NSERC; Discovery Grant to F.G.W) for funding. A.P. would like to thank the Chemistry-Biology Interface Training Program (T32 GM 008496) and the University of California, Los Angeles, for financial support. Computations were performed using the Hoffman2 cluster at the University of California, Los Angeles, as well as the Extreme Science and Engineering Discovery Environment's (TG CHE 040013N) Gordon and Trestles supercomputers at the San Diego Supercomputing Cluster.

## ■ REFERENCES

- (1) Benson, C. L.; West, F. G. *Org. Lett.* **2007**, *9*, 2545–2548.
- (2) Mazzola, R. D.; White, T. D.; Vollmer-Snarr, H. R.; West, F. G. *Org. Lett.* **2005**, *7*, 2799–2801.
- (3) Giese, S.; Mazzola, R. D.; Amann, C. M.; Arif, A. M.; West, F. G. *Angew. Chem., Int. Ed.* **2005**, *44*, 6546–6549.
- (4) Thomas, B. E.; Evanseck, J. D. *Isr. J. Chem.* **1993**, *3*, 287–293.
- (5) Evanseck, J. D.; Thomas, B. E.; Spellmeyer, D. C.; Houk, K. N. *J. Org. Chem.* **1995**, *60*, 7134–7141.
- (6) Walker, M. J.; Hietbrink, B. N.; Thomas, B. E.; Nakamura, K.; Kallel, E. A.; Houk, K. N. *J. Org. Chem.* **2001**, *66*, 6669–6672.
- (7) Guner, V. A.; Houk, K. N.; Davies, I. W. *J. Org. Chem.* **2004**, *69*, 8024–8028.
- (8) Leach, A. G.; Houk, K. N.; Davies, I. W. *Synthesis* **2005**, *19*, 3463–3467.
- (9) Patel, A.; Barcan, G. A.; Kwon, O.; Houk, K. N. *J. Am. Chem. Soc.* **2013**, *135*, 4878–4883.
- (10) Smith, D. A.; Ulmer, C. W., II. *J. Org. Chem.* **1991**, *56*, 4444–4447.
- (11) Smith, D. A.; Ulmer, C. W., II. *J. Org. Chem.* **1997**, *62*, 5110–5115.
- (12) Smith, D. A.; Ulmer, C. W., II. *Tetrahedron Lett.* **1991**, *32*, 725–728.
- (13) Cavalli, A.; Masetti, M.; Recanatini, M.; Prandi, C.; Guarna, A.; Occhiato, E. G. *Chemistry* **2006**, *12*, 2836–2845.
- (14) Lemière, G.; Gandon, V.; Cariou, K.; Fukuyama, T.; Dhimane, A.-L.; Fensterbank, L.; Malacria, M. *Org. Lett.* **2007**, *9*, 2207–2209.
- (15) Marcus, A. P.; Lee, A. S.; Davis, R. L.; Tantillo, D. J.; Sarpong, R. *Angew. Chem., Int. Ed.* **2008**, *47*, 6379–6383.
- (16) Lebœuf, D.; Huang, J.; Gandon, V.; Frontier, A. J. *Angew. Chem., Int. Ed.* **2011**, *50*, 10981–10985.

(17) Faza, O. N.; López, C. S.; Alvarez, R.; de Lera, A. R. *Chemistry* **2004**, *10*, 4324–4333.

(18) Harmata, M.; Schreiner, P. R.; Lee, D. R.; Kirchoefer, P. K. J. *Am. Chem. Soc.* **2004**, *126*, 10954–10957.

(19) Shi, F.-Q.; Li, X.; Xia, Y.; Zhang, L.; Yu, Z.-X. *J. Am. Chem. Soc.* **2007**, *129*, 15503–15512.

(20) Cavalli, A.; Pacetti, A.; Recanatini, M.; Prandi, C.; Scapi, D.; Occhiato, E. G. *Chem.—Eur. J.* **2008**, *14*, 9292–9304.

(21) Flynn, B. L.; Manchala, N.; Krenske, E. H. *J. Am. Chem. Soc.* **2013**, *135*, 9156–9163.

(22) Smith, D. A.; Ulmer, C. W., II. *J. Org. Chem.* **1993**, *58*, 4118–4121.

(23) Lebœuf, D.; Ciesielski, J.; Gandon, V.; Frontier, A. J. *J. Am. Chem. Soc.* **2012**, *134*, 6296–6308.

(24) Huang, J.; Lebœuf, D.; Frontier, A. J. *J. Am. Chem. Soc.* **2011**, *133*, 6307–6317.

(25) Lebœuf, D.; Theiste, E.; Gandon, V.; Daifuku, S. L.; Neidig, M. L.; Frontier, A. J. *Chem.—Eur. J.* **2013**, *19*, 4842–4848.

(26) Davies, D. I.; Parrott, M. J. *Tetrahedron Lett.* **1972**, *2*, 2719–2722.

(27) Baldwin, S. W.; Tomesch, J. C. *J. Org. Chem.* **1974**, *39*, 2382–2385.

(28) Freeman, F. *Chem. Rev.* **1975**, *75*, 439–490.

(29) Corey, E. J.; Shibasaki, M.; Nicolaou, K. C.; Malmsten, C. L.; Samuelsson, B. *Tetrahedron Lett.* **1976**, *17*, 737–740.

(30) Huisgen, R.; Ooms, P. H. J.; Mingin, M.; Allinger, N. L. *J. Am. Chem. Soc.* **1980**, *102*, 3951–3953.

(31) Huisgen, R. *Pure Appl. Chem.* **1981**, *53*, 171–187.

(32) Allen, A. D.; Tidwell, T. T. *J. Am. Chem. Soc.* **1982**, *104*, 3145–3149.

(33) von Ragué Schleyer, P. J. *Am. Chem. Soc.* **1967**, *89*, 701–703.

(34) Rondan, N. G.; Paddon-Row, M. N.; Caramella, P.; Mareda, J.; Mueller, P. H.; Houk, K. N. *J. Am. Chem. Soc.* **1982**, *104*, 4974–4976.

(35) Houk, K. N.; Rondan, N. G.; Brown, F. K.; Jorgensen, W. L.; Madura, J. D.; Spellmeyer, D. C. *J. Am. Chem. Soc.* **1983**, *105*, 5980–5988.

(36) Lopez, S. A.; Houk, K. N. *J. Org. Chem.* **2013**, *78*, 1778–1783.

(37) Wang, H.; Houk, K. N. *Chem. Sci.* **2014**, *5*, 462–470.

(38) Lewis, K. E.; Steiner, H. *J. Chem. Soc.* **1964**, 3080–3092.

(39) Krenske, E. H.; Perry, E. W.; Jerome, S. V.; Maimone, T. J.; Baran, P. S.; Houk, K. N. *Org. Lett.* **2012**, *14*, 3016–3019.

(40) In support of the notion that predistortion of bridged bicyclic alkenes promotes triene ring closures, Magomedov et al. have demonstrated that a norbornenyl divinyl ketone (in the presence of Lewis acid and an amine base) undergoes tautomerization followed by  $6\pi$  ring closure with greater yield and at lower temperatures than that for related acyclic or monocyclic substrates. For additional experimental details, see: Magomedov, N. A.; Ruggiero, P. L.; Tang, Y. *Org. Lett.* **2004**, *6*, 3373–3375.

(41) Shibasaki, K.; Fujii, A.; Mikami, N.; Tsuzuki, S. *J. Phys. Chem. A* **2006**, *110*, 4397–4404.

(42) Sherrill, C. D.; Takatani, T.; Hohenstein, E. G. *J. Phys. Chem. A* **2009**, *113*, 10146–10159.

(43) Dinadayalane, T. C.; Paytakov, G.; Leszczynski, J. *J. Mol. Model.* **2013**, *19*, 2855–2864.

(44) We chose the benzene–methane dimer as a rough measure of the strength of a CH  $\pi$  interaction because of the similarity in shape and size of benzene to the aromatic  $6\pi$  electron system in the electrocyclozation transition states. Differences in the aromaticities of the pericyclic transition state and benzene have little effect on the strength of  $\pi$  stacking. See Bloom, J. W. G.; Wheeler, S. E. *Angew. Chem., Int. Ed.* **2011**, *50*, 7847–7849. A similar point could be argued for CH  $\pi$  interactions, as the CH  $\pi$  dimer of ethylene and methane has a gas phase CCSD(T) complete basis set interaction energy of  $-0.5$  kcal mol<sup>-1</sup> very similar to the gas phase experimental interaction energy for the benzene–methane dimer of  $-1.0$  kcal mol<sup>-1</sup>. See ref 40 and Tsuzuki, S.; Honda, K.; Uchimaru, T.; Mikami, M.; Tanabe, K. *J. Phys. Chem. A* **1999**, *103*, 8265–8271.

(45) Frisch, M. J.; Trucks, G. W.; Schlegel, H. B.; Scuseria, G. E.; Robb, M. A.; Cheeseman, J. R.; Scalmani, G.; Barone, V.; Mennucci, B.; Petersson, G. A.; Nakatsuji, H.; Caricato, M.; Li, X.; Hratchian, H. P.; Izmaylov, A. F.; Bloino, J.; Zheng, G.; Sonnenberg, J. L.; Hada, M.; Ehara, M.; Toyota, K.; Fukuda, R.; Hasegawa, J.; Ishida, M.; Nakajima, T.; Honda, Y.; Kitao, O.; Nakai, H.; Vreven, T.; Montgomery, J. A., Jr.; Peralta, J. E.; Ogliaro, F.; Bearpark, M.; Heyd, J. J.; Brothers, E.; Kudin, K. N.; Staroverov, V. N.; Kobayashi, R.; Normand, J.; Raghavachari, K.; Rendell, A.; Burant, J. C.; Iyengar, S. S.; Tomasi, J.; Cossi, M.; Rega, N.; Millam, J. M.; Klene, M.; Knox, J. E.; Cross, J. B.; Bakken, V.; Adamo, C.; Jaramillo, J.; Gomperts, R.; Stratmann, R. E.; Yazyev, O.; Austin, A. J.; Cammi, R.; Pomelli, C.; Ochterski, J. W.; Martin, R. L.; Morokuma, K.; Zakrzewski, V. G.; Voth, G. A.; Salvador, P.; Dannenberg, J. J.; Dapprich, S.; Daniels, A. D.; Farkas, O.; Foresman, J. B.; Ortiz, J. V.; Cioslowski, J.; Fox, D. J. *Gaussian 09*, revision D.01; Gaussian, Inc.: Wallingford, CT, 2009.

(46) Zhao, Y.; Truhlar, D. G. *Theor. Chem. Acc.* **2008**, *120*, 215–241.

(47) Weigend, F.; Ahlrichs, R. *Phys. Chem. Chem. Phys.* **2005**, *7*, 3297–3305.

(48) Marenich, A. V.; Cramer, C. J.; Truhlar, D. G. *J. Phys. Chem. B* **2009**, *113*, 6378–6396.

(49) *The PyMOL Molecular Graphics System*, version 1.4; Schrödinger, LLC: New York.

(50) Dennington, R.; Keith, T.; Millam, J. *GaussView*, version 5; Semichem Inc.: Shawnee Mission, KS, 2009.

(51) *Avogadro: an open-source molecular builder and visualization tool*, version 1.1.1; <http://avogadro.openmolecules.net/>.

(52) Hanwell, M. D.; Curtis, D. E.; Lonie, D. C.; Vandermeersch, T.; Zurek, E.; Hutchison, G. R. *J. Cheminf.* **2012**, *4*, 17–17.

(53) Legault, C. Y. *CYLVview*, version 1.0b; Université de Sherbrooke: Sherbrooke, Quebec, Canada, 2009.